Proceedings of the 5th International Conference on Nonlinear Dynamics
ND-KhPI2016
September 27-30, 2016, Kharkov, Ukraine

Nonlinear vs Linear Models

Romashov Yu.[1,2*], Kizilova N.[2,3], Gaidulis G.[3]

Abstract
A tractable mathematical model of the valve dynamics is developed for the real time computations and in silico planning of the biomechanically consistent surgery on the ruptured chordae of the mitral valve. The geometry and dynamics of the heart contraction and valve closure are restored by digitization of the 2d echocardiography data measured on a patient. The chordae are modeled as branched systems of viscoelastic strings with zero bending rigidity. Both linear and nonlinear rheology of the heart tissues are considered. The corresponding numerical procedure is worked out. The developed model can be used for comparative study of different existing strategy of surgical restoration for individual patients as well as for fast real time computations of optimal location of the neochordae directly during the surgery.

Keywords
Biomechanics, mitral valve, chordae rupture, mitral insufficiency, surgery planning

[1] Kharkov National Polytechnic University 'KPI', Kharkov, Ukraine
[2] Kharkov National University, Kharkov, Ukraine
[3] Vilnius Gediminas Technical University, Vilnius, Lithuania
*** Corresponding author:** yu.v.romashov@gmail.com

Introduction

The mitral valve consists of two flexible leaflets located between the left atrium and ventricle. It provides unidirectional blood flow for the movements of the leaflets are restricted by a family of threads (chordae) connected the edges of the leaflets to the papillary muscles in the left ventricle. If the chordae are ruptured/overdistended or the edges are calcified, the mitral valve is not closed properly when the heart pumps out blood, so mitral insufficiency is developed. Surgical interventions are based on polytetrafluoroethylene (PTFE) neochorda reconstruction that influences the valve biomechanics. Unfortunately, in ~40-50% cases the surgery is unsuccessful and the intact chordae become overdistended or ruptured. Since the heart with its valves and chordae possess very complex geometry and biomechanics, the 2d and 3d modeling of its dynamics, computations of the stress-strain state, biomechanical interpretation of the numerical results, in silico planning and quantitative estimation of the outcome of surgery are needed.

The 3D geometry of the heart valves can be obtained using the 2d echocardiography (bottom view), but the walls, muscles and chordae remain invisible then. The side view gives a dynamic image of the heart chambers, papillary muscles and leaflets, but for the 2d modeling only. The multi row computed tomography gives a 3d image composed of the consequent series of the heart structures taken at the end of diastole or systolic peak. Location of the larger chordae can be approximated then by thicker regions over the valves. A series of 2d finite element models (FEMs) have been built and tested without the chordae [1], with a set of single chordae attached only along the edges of the leaflets [2]. The FEM computations are time consuming and geometry-dependent, therefore vast numerical computations are needed to follow the influence of different peculiarities of the normal/affected individual geometry and material parameters on the stress-strain state of the system modeled.

Special comparative analysis of the mass-spring (MS) and FEM valve models of the heart leaflets revealed the MS model is less accurate but approximately an order of magnitude faster than

the FE model [3]. Contrary to FEM, the MS model has no direct mechanism to control shear behavior. However, because the shear loading of the pressurized leaflets are much smaller than the normal forces experienced by them, the MS model approximates the deformations with small errors despite complex biomechanical properties of the leaflets [3].

In this paper a mathematical model of the valve dynamics is developed for *in silico* planning of the biomechanically consistent intervention and real time computations of the strain-stress state of the repaired valve. The chordae have been modeled as branched systems of linear/nonlinear elastic strings of different diameters without bending rigidity. The neochordae have been modeled as single PTFE threads connecting the edge of the leaflet to the corresponding papillary muscle. Displacements and stress-strain state of the chordae is determined by dynamics of the heart contraction restored from the 2d echocardiography records.

The developed model can be used for comparative study of different existing strategy of surgical restoration of the mitral valve for the individual patients as well as for fast real time computations of optimal location of the neochordae directly during the surgery. The proposed approach will be validated on a group of patients recommended for the mitral valve restoration.

1. Geometry and function of the valve leaflets and chordae

During the heart contraction the blood moves through the open mitral valve from the left atrium into the ventricle [4]. In the open state the chordae are not stretched. While the blood pressure in the ventricle increases, the reverse blood flow closes the leaflets and the stretched chordae (1 in Fig.1a) prevents the leaflets (2 in Fig.1a) from opening outside the ventricle (4 in Fig.1a). The primary chordae are attached at the very edge of the leaflets, while the secondary chordae are attached along the ~1/2-2/3 of the leaftels' surface (5 in Fig.1b). Some chordae are presented by branched structures with segments and nodes (8 and 7 in Fig.1b) but the opposite ends of all the chordae are attached to the papillary muscles (3 in Fig.1a, 6 in Fig.1b). The branches provide more uniform stress distribution over the leaflets which are composed by several thin layers of connective tissue [4].

Due to diseases and/or age-related tissue degeneration some chordae could be overdistensed or even ruptured. In those cases the valves are not tightly closed during the cardic cycle and some amount of blood returns back into the atrium. In some patients due to the myocardial infarction the papillary muscles are located too low and the chordae are overstretched that restricted the valve dynamics and could promote the rupture. Individual geometry of the heart chambers and dynamics of the leaflets and papillary muscles movement during the cardiac cycle could be easily restored from the high resolution ultrasound records, while geometry of the chordae are not clearly visible even on the more detailed CT images. In that way, investigation of the influence of individual geometry of the chordae branching and location over the leaflets on the strain-stress distribution in the system is of great interest for biomechanical analysis of the neochordae location and, therefore, surgery planning. Location of the nodes of branching, length and thickness of the chordae branching (Fig.1b) must be studied for each individual geometry of chambers and desirable valve dynamics.

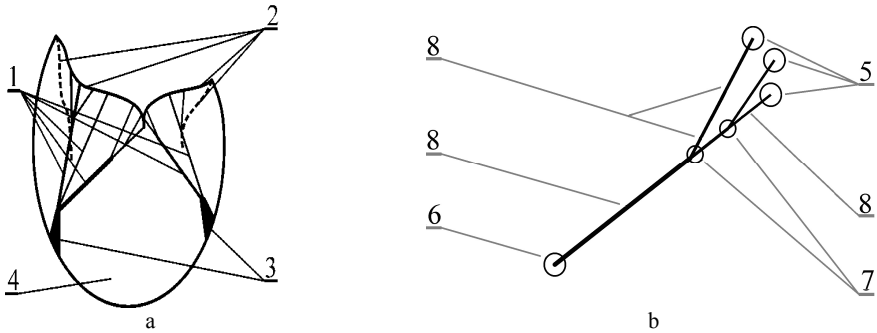

Figure 1. Structure of the left ventricle (a) and chordae branching (b). Here 1 – chordae; 2 – alterior (left) and posterior (right) valve leaflets in a closed (solid lines) and open (dashed lines) states; 3 – papillary muscles; 4 – left ventricle; 5 – chorda edges at the leaflet and 6 – at the papillary muscle surfaces; 7 – branching nodes; 7-8 – chordae of the 1-st, 2-nd and 3-rd branching orders.

2. Mathematical formulation of the chordae dynamics

Heart tissues (walls, muscles and leaflets) and chordae are treated as combined mechanical systems with different properties that allows separate consideration of the heart biomechanics and dynamics of the chordae.

2.1 Influence of the chordae on the heart tissues

Let us consider the heart (without) chordae as a holonomic mechanical systems with some finite degrees of freedom (DOF) and the generalized coordinates q_p, $p = 1,2,\ldots$. Then the heart movement can be presented in the form of the Lagrange's equations of the second kind:

$$\frac{d}{dt}\frac{\partial L}{\partial \dot{q}_p} - \frac{\partial L}{\partial q_p} = \hat{Q}_p + \widetilde{Q}_p \tag{1}$$

where L is the Lagrance function for the heart muscle, $\hat{Q}_p$ are generalized forces produced by action of the moving chordae on the heart, $\widetilde{Q}_p$ are generalized forces produced by other factors.

As it follows from (1), the modeling of mechanical behavior of the chordae is reduced to determination of the generalized forces $\hat{Q}_p$, $p = 1,2,\ldots$. Let us describe the individual geometry of the chordae by the index $s = 1,2,\ldots$ (Fig. 2a). It is assumed the chorda s has $\mu^{(s)}$ ends numerated as $i = 1,2,\ldots,\mu^{(s)}$; location of each chorda is determined by the position vectors $\vec{\rho}_i^{(s)}$ (Fig. 2b). When the valve is open, the chordae are not stretched and slack, that means the interaction of them with the heart are determined by the main force vector directed along the corresponding rectilinear segment, while the net moment of force in the attachment nodes (5 in Fig.1b) is zero. Let us denote as $\vec{\Phi}_i^{(s)}$ the main force vectors acting onto the heart and applied in the nodes $i = 1,2,\ldots,\mu^{(s)}$ (Fig. 2b). Now one can calculate the generalized forces $\hat{Q}_p$, $p = 1,2,\ldots$ from the virtual work $\delta\hat{A}$ produced by the forces $\vec{\Phi}_i^{(s)}$, $i = 1,2,\ldots,\mu^{(s)}$ of all the chordae $s = 1,2,\ldots$ attached to both leaflets

$$\delta\hat{A} = \sum_{s=1,2,\ldots} \sum_{i=1}^{\mu^{(s)}} \vec{\Phi}_i^{(s)} \cdot \delta\vec{\rho}_i^{(s)} \tag{2}$$

where $\delta\vec{\rho}_i^{(s)}$ are virtual displacements of the chordae ends.

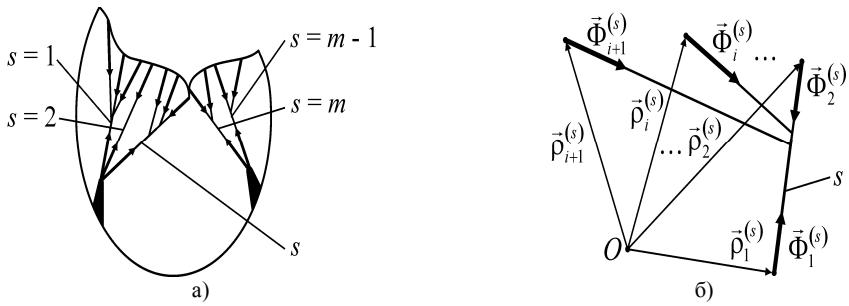

Figure 2. An example of individual geometry of the chordae (a) and the forces produced by them at the leaflet and papillary muscle (b); $s = 1,2,\ldots$ are ordinal numbers of the chordae

Since locations of the ends of the chordae coincide with contracting heart tissues, the position vectors $\vec{\rho}_i^{(s)}$ could be defined via the generalized coordinates q_p assuming the constraints between the chordae and tissues are stationary: $\vec{\rho}_i^{(s)} = \vec{\rho}_i^{(s)}\left(q_1, q_2, \ldots, q_p, \ldots\right)$. Then after some transformations of (2) one can obtain the generalized forces in the form

$$\hat{Q}_p = \sum_{s=1,2,\ldots} \sum_{i=1}^{\mu^{(s)}} \vec{\Phi}_i^{(s)} \cdot \frac{\partial \vec{\rho}_i^{(s)}}{\partial q_p} \tag{3}$$

As it is clear from (3), foe determination of $\hat{Q}_p$ one needs to know the expressions for $\vec{\Phi}_i^{(s)}$, which are determined by movement and deformation of the chordae.

2.2 Modeling the rectilinear segments of the chordae as deformable threads

The chordae are considered here as elastic threads (Fig.3) with relatively high Young's modulus but zero bending rigidity [5,6]. They are able to sustain quite high stresses produced by the blood pressure in the heart chambers but easily bended and slack when the valve is open. The current length of the thread in the stretched state can be described by the distance between its ends A and B determined by their positional vectors $\vec{r}_A$ and $\vec{r}_B$ (Fig. 3). Then the length and the elongation rate of the thread are

$$\begin{cases} l = \sqrt{(\vec{r}_B - \vec{r}_A)\cdot(\vec{r}_B - \vec{r}_A)} \\ \dot{l} = (\vec{r}_B - \vec{r}_A)\cdot(\dot{\vec{r}}_B - \dot{\vec{r}}_A) \Big/ \sqrt{(\vec{r}_B - \vec{r}_A)\cdot(\vec{r}_B - \vec{r}_A)} \end{cases} \tag{4}$$

Alongside with the geometric constraints (4), we assume the internal forces acting at any infinitesimal segment SS' ($dl << |AB|$) of the thread on its cross sections S and S' are equivalent to the main force vectors $\vec{F}$ and $\vec{F}'$ directed along the thread in its current position where $\vec{F}' = -\vec{F}$ (Fig. 3). The forces $\vec{F}_A$ and $\vec{F}_B$ at the ends A and B of the thread нити satisfies the same condition $\vec{F}_B = -\vec{F}_A$. Due to zero bending rigidity of the threads, the forces $\vec{F}, \vec{F}'$, $\vec{F}_A$, $\vec{F}_B$ are purely stretching ones. The main vectors of internal forces have the same value $F = |\vec{F}|$ in each cross section of the stretched thread and is called the tensile force.

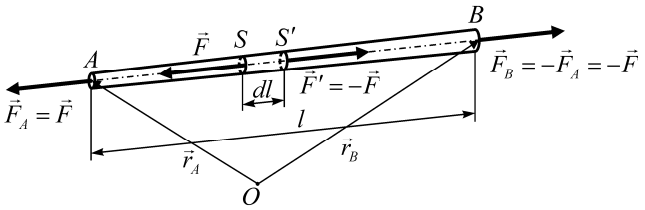

Figure 3. A stretched thread and its internal forces

Mechanical behavior of the viscoelastic thread is described by the dependence

$$F = F\left(l - l_0, \dot{l}\right) \tag{5}$$

where l_0 is its length in the unloaded (undeformed) state.

As it follows from (4) and (5) the tensile force is the function of the initial length, current coordinates and elongation rate

$$F = F\left(\vec{r}_A, \vec{r}_B, \dot{\vec{r}}_A, \dot{\vec{r}}_B; l_0\right) \tag{6}$$

Note that (6) is a nonlinear function even when the linear elasticity model is accepted for the thread material.

2.3 Modeling the mechanical behavior of the rectilinear threads

In the simplest case the chorda possess two ends attached to the papillary muscle and the leaflet accordingly (e.g. the chorda $s = 2$ in Fig.2a) and $\mu^{(s)} = 2$ (Fig.4a). The mechanical behavior of such chordae is only determined by the law (5). Indeed, in the case $\mu^{(s)} = 2$ the forces produced by the chorda *s* at the heart are functions of its tensile force (Fig. 4a):

$$\begin{cases} \vec{\Phi}_1^{(s)} = \Phi^{(s)}\left(\vec{\rho}_1, \vec{\rho}_2, \dot{\vec{\rho}}_1, \dot{\vec{\rho}}_2; l_0^{(s)}\right) \dfrac{\vec{\rho}_2 - \vec{\rho}_1}{\sqrt{(\vec{\rho}_2 - \vec{\rho}_1)\cdot(\vec{\rho}_2 - \vec{\rho}_1)}} \\ \vec{\Phi}_2^{(s)} = -\vec{\Phi}_1^{(s)} \end{cases} \tag{7}$$

where $\Phi^{(s)}\left(\vec{\rho}_1, \vec{\rho}_2, \dot{\vec{\rho}}_1, \dot{\vec{\rho}}_2; l_0^{(s)}\right)$ is the mechanical law for the chorda expressed in the form (6).

The expressions (7) are needed for computations of the generalized forces $\hat{Q}_p$ by (3). When all the chordae are rectilinear (Fig.4a), one can obtain the expressions (7) written for each chorda which gives the system of nonlinear equations for determination of the generalized forces as it is acceptable for holonomic systems [7].

2.4 Modeling the mechanical behavior of the branched threads

The branched chordae can be considered as a system of elastic threads attached in a set of nodes (Fig.1b). The forces appeared in the nodes are directed along the stretched segments and obey the Newton's third law of motion. An example of the force distribution is presented in Fig.4b for $\mu^{(s)} = 4$. In the internal segments attached to neither papillary muscle nor leaflet, the internal tensile forces $\vec{N}_1^{(s)}$ appear. In a general case we have $m^{(s)}$ nodes determined by the position vectors $\vec{r}_j^{(s)}$ numerated by the index $j = 1,2,\ldots,m^{(s)}$, as well as $\nu^{(s)}$ internal segments experiencing the tensile forces $\vec{N}_k^{(s)}$, $k = 1,2,\ldots,\nu^{(s)}$.

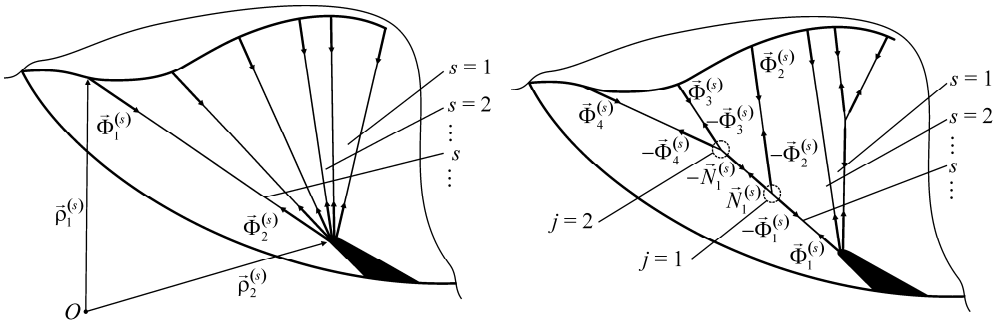

а) б)

Figure 4. A leaflet with a set of 6 rectilinear chordae (a) and with 1 rectilinear and 2 branched chordae (б)

Let us denote $J^{(s)}(i)$ is the ordinal number of the node connected to the end $i \in 1,2,\ldots,\mu^{(s)}$ of the chorda s. Similarly, $J_1^{(s)}(k)$ and $J_2^{(s)}(k)$ are the ordinal numbers of the nodes of the chorda s which are connected to the internal segment number $k \in 1,2,\ldots,\nu^{(s)}$. $\vec{N}_k^{(s)}$ and $-\vec{N}_k^{(s)}$ are the forces acting in the nodes with numbers $J_1^{(s)}(k)$ and $J_2^{(s)}(k)$ accordingly. Then the forces $\vec{\Phi}_i^{(s)}$, $i = 1,2,\ldots,\mu^{(s)}$ and $\vec{N}_k^{(s)}$, $k = 1,2,\ldots,\nu^{(s)}$ can be computed as following:

$$\vec{\Phi}_i^{(s)} = \Phi_i^{(s)}\left(\vec{\rho}_i^{(s)}, \vec{r}_{J^{(s)}(i)}^{(s)}, \dot{\vec{\rho}}_i^{(s)}, \dot{\vec{r}}_{J^{(s)}(i)}^{(s)}; \lambda_{i0}^{(s)}\right) \frac{\vec{\rho}_i^{(s)} - \vec{r}_{J^{(s)}(i)}^{(s)}}{\sqrt{\left(\vec{\rho}_i^{(s)} - \vec{r}_{J^{(s)}(i)}^{(s)}\right)\cdot\left(\vec{\rho}_i^{(s)} - \vec{r}_{J^{(s)}(i)}^{(s)}\right)}} \tag{8}$$

$$\vec{N}_k^{(s)} = N_k^{(s)}\left(\vec{r}_{J_1^{(s)}(k)}^{(s)}, \vec{r}_{J_2^{(s)}(k)}^{(s)}, \dot{\vec{r}}_{J_1^{(s)}(k)}^{(s)}, \dot{\vec{r}}_{J_2^{(s)}(k)}^{(s)}; l_{k0}^{(s)}\right) \frac{\vec{r}_{J_2^{(s)}(k)}^{(s)} - \vec{r}_{J_1^{(s)}(k)}^{(s)}}{\sqrt{\left(\vec{r}_{J_2^{(s)}(k)}^{(s)} - \vec{r}_{J_1^{(s)}(k)}^{(s)}\right)\cdot\left(\vec{r}_{J_2^{(s)}(k)}^{(s)} - \vec{r}_{J_1^{(s)}(k)}^{(s)}\right)}} \tag{9}$$

where $\Phi_i^{(s)}\left(\vec{\rho}_i^{(s)}, \vec{r}_{J^{(s)}(i)}^{(s)}, \dot{\rho}_i^{(s)}, \dot{\vec{r}}_{J^{(s)}(i)}^{(s)}; \lambda_{i0}^{(s)}\right)$ and $\lambda_{i0}^{(s)}$ are the dynamics law and initial undisturbed length of the corresponding marginal segment, $N_k^{(s)}\left(\vec{r}_{J_1^{(s)}(k)}^{(s)}, \vec{r}_{J_2^{(s)}(k)}^{(s)}, \dot{\vec{r}}_{J_1^{(s)}(k)}^{(s)}, \dot{\vec{r}}_{J_2^{(s)}(k)}^{(s)}; l_{k0}^{(s)}\right)$ and $l_{i0}^{(s)}$ are the dynamics law and initial undisturbed length of the corresponding internal segment.

Since $\vec{\rho}_i^{(s)} = \vec{\rho}_i^{(s)}\left(q_1, q_2, \ldots, q_p, \ldots\right)$, the forces (8) can be determined as

$$\vec{\Phi}_i^{(s)} = \vec{\Phi}_i^{(s)}\left(q_1, q_2, \ldots, \dot{q}_1, \dot{q}_2, \ldots, \vec{r}_{J^{(s)}(i)}^{(s)}, \dot{\vec{r}}_{J^{(s)}(i)}^{(s)}\right) \tag{10}$$

After substitution (10) into (3), one can obtain the following expressions for the generalized forces as functions of the generalized coordinates of the heart tissues and chordae and their time derivatives

$$\hat{Q}_p = \hat{Q}_p\left(q_1, q_2, \ldots, \dot{q}_1, \dot{q}_2, \ldots, \vec{r}_1^{(s)}, \ldots, \vec{r}_{m^{(s)}}^{(s)}, \dot{\vec{r}}_1^{(s)}, \ldots, \dot{\vec{r}}_{m^{(s)}}^{(s)}\right) \tag{11}$$

in which all the structures $s = 1,2,\ldots$ are taken into account.

Since the chordae are thing threads and their mass is negligibly small in comparison to the heart tissues mass, the movement of the nodes is determined by the Newton's second law of motion in the matrix form:

$$\sum_{i=1}^{\mu^{(s)}} M_{ji}^{(s)} \vec{\Phi}_i^{(s)} + \sum_{k=1}^{\nu^{(s)}} \Lambda_{jk}^{(s)} \vec{N}_k^{(s)} = \vec{0} \qquad j = 1,2,\ldots,m^{(s)} \tag{12}$$

where $M_{ji}^{(s)}$ и $\Lambda_{jk}^{(s)}$ are the matrices determined by geometry of the branched chordae.

Substituting (9), (10) into (12), we obtain the differential relationships which at known generalized coordinates $q_1, q_2, \ldots$ determined by the heart contraction can be considered as differential equations for determination of the position vectors $\vec{r}_j^{(s)}$, $j = 1,2,\ldots,m^{(s)}$ of the nodes. Therefore, the proposed mathematical model of heart biomechanics includes the Lagrange's equations (1) for the heart tissues, that, accounting for (11) are coupled and must be integrated together with differential equations for displacements of the nodes (8), (9), (12).

3. Analysis of mechanical behavior of the branched chordae

Generally the chordae are composed of viasoelastic materials which obey, but in some cases the viscous forces could be small in comparison to the elastic deformations. The elastic deformation is described by the function

$$F = F\left(l - l_0\right), \tag{13}$$

which is a particular case of (5).

Accounting for (13), we may accept instead (8), (9) the following expressions:

$$\begin{cases} \vec{\Phi}_i^{(s)} = \Phi_i^{(s)}\left(\vec{\rho}_i^{(s)}, \vec{r}_{J^{(s)}(i)}^{(s)}; \lambda_{i0}^{(s)}\right) \dfrac{\vec{\rho}_i^{(s)} - \vec{r}_{J^{(s)}(i)}^{(s)}}{\sqrt{\left(\vec{\rho}_i^{(s)} - \vec{r}_{J^{(s)}(i)}^{(s)}\right) \cdot \left(\vec{\rho}_i^{(s)} - \vec{r}_{J^{(s)}(i)}^{(s)}\right)}} \\ \vec{N}_k^{(s)} = N_k^{(s)}\left(\vec{r}_{J_1^{(s)}(k)}^{(s)}, \vec{r}_{J_2^{(s)}(k)}^{(s)}; l_{k0}^{(s)}\right) \dfrac{\vec{r}_{J_2^{(s)}(k)}^{(s)} - \vec{r}_{J_1^{(s)}(k)}^{(s)}}{\sqrt{\left(\vec{r}_{J_2^{(s)}(k)}^{(s)} - \vec{r}_{J_1^{(s)}(k)}^{(s)}\right) \cdot \left(\vec{r}_{J_2^{(s)}(k)}^{(s)} - \vec{r}_{J_1^{(s)}(k)}^{(s)}\right)}} \end{cases} \tag{14}$$

For the linear elasticity the law (13) and expression (14) have the form:

$$F = c\left(l - l_0\right) \tag{15}$$

$$\begin{cases} \vec{\Phi}_i^{(s)} = \gamma_i^{(s)}\left(\sqrt{\left(\vec{\rho}_i^{(s)} - \vec{r}_{J^{(s)}(i)}^{(s)}\right)\cdot\left(\vec{\rho}_i^{(s)} - \vec{r}_{J^{(s)}(i)}^{(s)}\right)} - \lambda_{i0}^{(s)}\right)\dfrac{\vec{\rho}_i^{(s)} - \vec{r}_{J^{(s)}(i)}^{(s)}}{\sqrt{\left(\vec{\rho}_i^{(s)} - \vec{r}_{J^{(s)}(i)}^{(s)}\right)\cdot\left(\vec{\rho}_i^{(s)} - \vec{r}_{J^{(s)}(i)}^{(s)}\right)}} \\ \vec{N}_k^{(s)} = c_k^{(s)}\left(\sqrt{\left(\vec{r}_{J_2^{(s)}(k)}^{(s)} - \vec{r}_{J_1^{(s)}(k)}^{(s)}\right)\cdot\left(\vec{r}_{J_2^{(s)}(k)}^{(s)} - \vec{r}_{J_1^{(s)}(k)}^{(s)}\right)} - l_{k0}^{(s)}\right)\dfrac{\vec{r}_{J_2^{(s)}(k)}^{(s)} - \vec{r}_{J_1^{(s)}(k)}^{(s)}}{\sqrt{\left(\vec{r}_{J_2^{(s)}(k)}^{(s)} - \vec{r}_{J_1^{(s)}(k)}^{(s)}\right)\cdot\left(\vec{r}_{J_2^{(s)}(k)}^{(s)} - \vec{r}_{J_1^{(s)}(k)}^{(s)}\right)}} \end{cases} \tag{16}$$

where c is the rigidity coefficient for the thread, $\gamma_i^{(s)}$ and $c_k^{(s)}$ are stiffness of the marginal and internal nodes of the branched chordae accordingly.

Substituting (16) into (12), we obtain the mathematical model of the linear elastic weightless chorda. The model is presented as a system of non-linear algebraic equations for determination of locations of the nodes governed by the known movement of the heart tissues. Let us consider the mechanical behavior of the chorda with one internal node (Fig.5). In this case $\mu^{(s)} = 3$, $m^{(s)} = 1$, $\nu^{(s)} = 0$, matrix $M_{ji}^{(s)} = \begin{pmatrix} -1 & -1 & -1 \end{pmatrix}$, and the expressions (16) have the form:

$$\vec{\Phi}_i^{(s)} = \frac{\gamma_i^{(s)}\left(\sqrt{\left(\xi_i^{(s)} - x_1^{(s)}\right)^2 + \left(\eta_i^{(s)} - y_1^{(s)}\right)^2} - \lambda_{i0}^{(s)}\right)}{\sqrt{\left(\xi_i^{(s)} - x_1^{(s)}\right)^2 + \left(\eta_i^{(s)} - y_1^{(s)}\right)^2}}\left(\left(\xi_i^{(s)} - x_1^{(s)}\right)\vec{i} + \left(\eta_i^{(s)} - y_1^{(s)}\right)\vec{j}\right) \tag{17}$$

where $\xi_i^{(s)}$ and $\eta_i^{(s)}$ are coordinates of the ends of the chorda, $(x_1^{(s)}, y_1^{(s)})$ are coordinates of its nodes, $\vec{i}$ and $\vec{j}$ are unit vectors of the coordinates (x,y).

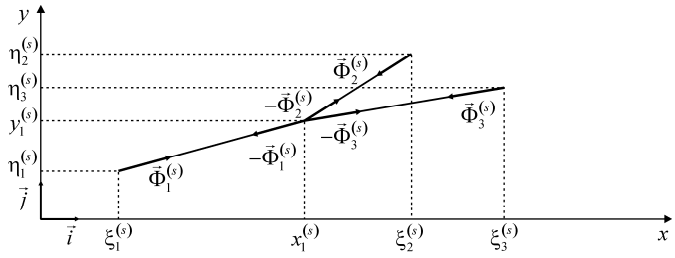

Figure 5. An example of chorda with one branching mode

Then from (17) one can obtain the nonlinear system of two equations for determination the coordinates of the only internal node $(x_1^{(s)}, y_1^{(s)})$ in the form:

$$\begin{cases} -x_1^{(s)}\sum\limits_{i=1}^{3}\gamma_i^{(s)} + \sum\limits_{i=1}^{3}\gamma_i^{(s)}\xi_i^{(s)} = \sum\limits_{i=1}^{3}\dfrac{\gamma_i^{(s)}\lambda_{i0}^{(s)}\left(\xi_i^{(s)} - x_1^{(s)}\right)}{\sqrt{\left(\xi_i^{(s)} - x_1^{(s)}\right)^2 + \left(\eta_i^{(s)} - y_1^{(s)}\right)^2}} - 2\dfrac{\gamma_1^{(s)}\lambda_{10}^{(s)}\left(\xi_1^{(s)} - x_1^{(s)}\right)}{\sqrt{\left(\xi_1^{(s)} - x_1^{(s)}\right)^2 + \left(\eta_1^{(s)} - y_1^{(s)}\right)^2}} \\ -y_1^{(s)}\sum\limits_{i=1}^{3}\gamma_i^{(s)} + \sum\limits_{i=1}^{3}\gamma_i^{(s)}\eta_i^{(s)} = \sum\limits_{i=1}^{3}\dfrac{\gamma_i^{(s)}\lambda_{i0}^{(s)}\left(\eta_i^{(s)} - y_1^{(s)}\right)}{\sqrt{\left(\xi_i^{(s)} - y_1^{(s)}\right)^2 + \left(\eta_i^{(s)} - y_1^{(s)}\right)^2}} - 2\dfrac{\gamma_1^{(s)}\lambda_{10}^{(s)}\left(\eta_i^{(s)} - y_1^{(s)}\right)}{\sqrt{\left(\xi_1^{(s)} - x_1^{(s)}\right)^2 + \left(\eta_1^{(s)} - y_1^{(s)}\right)^2}} \end{cases} \tag{18}$$

where the coordinates of $(\xi_i^{(s)}, \eta_i^{(s)})$ of the fastening points are known from the measurement data of the papillary muscle (s=1) and two points of the leaflet (s=2,3) location at each instant time. Solution

of (18) could be easily obtained by using the Newtons method with initial approximation of the solution in the linear form $x_1^{(s)} = \sum_{i=1}^{3} \gamma_i^{(s)} \xi_i^{(s)} \Big/ \sum_{i=1}^{3} \gamma_i^{(s)}$, $y_1^{(s)} = \sum_{i=1}^{3} \gamma_i^{(s)} \eta_i^{(s)} \Big/ \sum_{i=1}^{3} \gamma_i^{(s)}$.

The computation results may be validated by comparative analysis of the computed displacements of the nodes and the in vivo detected locations of the radiopaque beads introduced into the heart structures and nodes in acute experiment on animals [8] or direct measurements of the tensile stressed along the chordae/neochordae in the contracting heart in vitro [9].

Conclusions

In the proposed tractable model the heart tissues (walls, muscles, leaflets) and the chordae are considered as two coupled mechanical systems. Detailed data on motion of the papillary muscle and leaflets can be easily obtained from 2d echocardiography images of the heart contraction. The leaflets in the side view are visible as smoothed polyline, while the papillary muscles are seen as moving points. The coordinates of the digitized structures provide the boundary conditions for the marginal ends of the chordae fastened to the papillary muscles and leaflets. Then the location of the internal nodes of the chordae and the stress-strain distributions in the segments can be computed from the Newton's second law of motion. The problem is reduced to a set of non-linear algebraic equations for computations of coordinates of the internal nodes. Then the stretching forces in the chordae could be computed from the rheological laws for elastic or viscoelastic chordae and compared to the critical values close to the ultimate tensile strength of the chords of given thickness and age-related degradation level or calcification. The model is simple and fast and can be useful for not only preliminary in silico planning of locations and lengths of the neochordas, but also for the real time correcting computations during the surgery.

References

[1] Votta E., Caiani E., Veronesi F., et al. Mitral valve finite-element modelling from ultrasound data: a pilot study for a new approach to understand mitral function and clinical scenarios. *Philosophical Transactions of the Royal Society, Ser.A*, Vol. 366, pp. 3411–3434, 2008.

[2] Votta E., Le T.B., Stevanella M., et al. Toward patient-specific simulations of cardiac valves: State-of-the-art and future directions. *Journal of Biomechanics*, Vol. 46, pp. 217–228, 2013.

[3] Hammer P.E., Sacks M.S., del Nido P.J., Howe R.D. Mass-spring vs. finite element models of anisotropic heart valves: speed and accuracy. *Proceedings of the ASME Summer Bioengineering Conference* (SBC2010), Naples Florida, USA, 2010.

[4] Feigenbaum H., Armstrong W.F., Ryan Th. *Feigenbaum's Echocardiography, 6th ed.*, Philadelphia: Lippincott Williams & Wilkins, 876 p., 2004.

[5] Appel P. *Theoretical mechanics. Vol.1. Statics. Dynamics of point*. Moscow, Fizmatgiz, 1960 (in Russian).

[6] Levi-Civita T., Amaldi U. *Theoretical mechanics. Vol.1. Kinematics. Principles of mechanics. Statics*. Moscow, MIR, 1952, 326 p., 1952 (in Russian).

[7] Gantmacher F.R. *Lectures on analytical mechanics. 2-nd ed.*, Moscow, Nauka, 300 p., 1966 (in Russian).

[8] Rodriguez F., Langer F., Harrington K.B., et al. Importance of mitral valve second-order chordae for left ventricular geometry, wall thickening mechanics, and global systolic function. *Circulation*, Vol. 110 (suppl II), pp. 115-122, 2004.

[9] Bajona P., Zehr K.J., Liao J., Speziali G. Tension Measurement of Artificial Chordae Tendinae Implanted Between the Anterior Mitral Valve Leaflet and the Left Ventricular Apex. *Innovations*, Vol. 3(1), pp. 33-37, 2008.